



AFRL-RX-WP-JA-2021-0081

**HYBRID MATERIAL DESIGN ISSUES AND
CHALLENGES FOR MATERIALS FUNCTIONALITY
FOR MICRODEVICES (POSTPRINT)**

Ajit K. Roy

AFRL/RXAN

16 November 2020

Interim Report

**DISTRIBUTION STATEMENT A.
Approved for public release: distribution is unlimited.**

© 2021 ELSEVIER INC.

**(STINFO COPY)
AIR FORCE RESEARCH LABORATORY
MATERIALS AND MANUFACTURING DIRECTORATE
WRIGHT-PATTERSON AIR FORCE BASE, OH 45433-7750
AIR FORCE MATERIEL COMMAND
UNITED STATES AIR FORCE**

REPORT DOCUMENTATION PAGE

Form Approved
OMB No. 0704-0188

The public reporting burden for this collection of information is estimated to average 1 hour per response, including the time for reviewing instructions, searching existing data sources, gathering and maintaining the data needed, and completing and reviewing the collection of information. Send comments regarding this burden estimate or any other aspect of this collection of information, including suggestions for reducing this burden, to Department of Defense, Washington Headquarters Services, Directorate for Information Operations and Reports (0704-0188), 1215 Jefferson Davis Highway, Suite 1204, Arlington, VA 22202-4302. Respondents should be aware that notwithstanding any other provision of law, no person shall be subject to any penalty for failing to comply with a collection of information if it does not display a currently valid OMB control number. **PLEASE DO NOT RETURN YOUR FORM TO THE ABOVE ADDRESS.**

1. REPORT DATE (DD-MM-YY) 16 November 2020		2. REPORT TYPE Interim		3. DATES COVERED (From - To) 16 April 2020 – 16 October 2020	
4. TITLE AND SUBTITLE Hybrid Material Design Issues and Challenges for Materials Functionality for Microdevices (Postprint)				5a. CONTRACT NUMBER In House	
				5b. GRANT NUMBER	
				5c. PROGRAM ELEMENT NUMBER	
6. AUTHOR(S) Ajit K. Roy – AFRL/RXAN (Continued on next page)				5d. PROJECT NUMBER	
				5e. TASK NUMBER	
				5f. WORK UNIT NUMBER X1SQ	
7. PERFORMING ORGANIZATION NAME(S) AND ADDRESS(ES) AFRL/RX 2977 Hobson Way Wright-Patterson AFB OH 45433 (Continued on next page)				8. PERFORMING ORGANIZATION REPORT NUMBER	
9. SPONSORING/MONITORING AGENCY NAME(S) AND ADDRESS(ES) Air Force Research Laboratory Materials and Manufacturing Directorate Wright-Patterson Air Force Base, OH 45433-7750 Air Force Materiel Command United States Air Force				10. SPONSORING/MONITORING AGENCY ACRONYM(S) AFRL/RXAN	
				11. SPONSORING/MONITORING AGENCY REPORT NUMBER(S) AFRL-RX-WP-JA-2021-0081	
12. DISTRIBUTION/AVAILABILITY STATEMENT DISTRIBUTION STATEMENT A. Approved for public release: distribution is unlimited.					
13. SUPPLEMENTARY NOTES PA Case Number: AFRL-2020-0288; Clearance Date: 16 Nov2020. This document contains color. Journal article published in Hybrid Atomic-Scale Interface Design for Materials Functionality, online 19 Mar 2021. © 2021 Elsevier Inc. The U.S. Government is joint author of the work and has the right to use, modify, reproduce, release, perform, display, or disclose the work. The final publication is available at https://doi.org/10.1016/B978-0-12-819117-0.00011-5					
14. ABSTRACT (Maximum 200 words) It is well-known fact that materials are the enabler to advancing quality of life and associated machines, devices and its technology—touching essentially every aspect of technology spectrum—bio and healthcare, wearable sensors, transportation, consumer products, and defense industry. The technology advancement in the devices (bio, healthcare, energy managements, sensors, etc.) that we use in our way of life is essentially measured by its performance efficiency. There is a logical expectation as well as demand for enhanced performance efficiency of the devices, as we move forward with technology advancement with time. Here, materials are an integral component and without any argument is the kernel enabler toward advancing the performance efficiency of devices, machinery, etc. Increase in device performance efficiency is invariably tied with its materials that is to work (perform) more per its unit mass usage. In pursuit of increasing performance efficiency, materials in future are expected to perform in complex and dynamic environments, and efficient materials often exhibit simultaneous multifunctionality (structural, electrical, thermal, optical, etc.), even in very dynamic environment.					
15. SUBJECT TERMS Materials; design; efficiency; fullerene; nanoparticles; conductance					
16. SECURITY CLASSIFICATION OF:			17. LIMITATION OF ABSTRACT: SAR	18. NUMBER OF PAGES 20	19a. NAME OF RESPONSIBLE PERSON (Monitor) Marc Martin 19b. TELEPHONE NUMBER (Include Area Code) (937) 255-9645
a. REPORT Unclassified	b. ABSTRACT Unclassified	c. THIS PAGE Unclassified			

REPORT DOCUMENTATION PAGE Cont'd

6. AUTHOR(S)

Ajit K. Roy - AFRL/RXAN

7. PERFORMING ORGANIZATION NAME(S) AND ADDRESS(ES)

AFRL/RX
2977 Hobson Way
Wright-Patterson AFB OH 45433

Hybrid material design issues and challenges for materials functionality for microdevices

Ajit K. Roy

Materials and Manufacturing Directorate, Air Force Research Laboratory, Wright-Patterson AFB, Dayton, OH, United States

1.1 Introduction

It is well-known fact that materials are the enabler to advancing quality of life and associated machines, devices and its technology—touching essentially every aspect of technology spectrum—bio and healthcare, wearable sensors, transportation, consumer products, and defense industry.^{1–8} The technology advancement in the devices (bio, healthcare, energy managements, sensors, etc.) that we use in our way of life is essentially measured by its performance efficiency. There is a logical expectation as well as demand for enhanced performance efficiency of the devices, as we move forward with technology advancement with time. Here, materials are an integral component and without any argument is the kernel enabler toward advancing the performance efficiency of devices, machinery, etc. Increase in device performance efficiency is invariably tied with its materials that is to work (perform) more per its unit mass usage. In pursuit of increasing performance efficiency, materials in future are expected to perform in complex and dynamic environments, and efficient materials often exhibit simultaneous multifunctionality (structural, electrical, thermal, optical, etc.), even in very dynamic environment.

Hybrid materials design (i.e., materials hybridization), in contrary to monolithic material design concept, offers efficient materials usage to meet any given performance objective at reduced materials use. For example, in the case of a monolithic material design, a device component working under a gradient field would not necessarily be able to extract same amount of work at every point of materials volume. Whereas, placing materials type of choice selectively at different locations (i.e., materials hybridization) to extract almost same amount of work pointwise would boost overall materials performance and hence device performance efficiency. Also, the materials interfaces and its local materials morphology play a crucial role in the hybrid materials design and in realizing the desired performance characteristics.^{9,10} Further, materials hybridization at smaller scale,

as such at atomic scale, offers exceedingly high-payoff opportunities for optimizing materials functionality at reduced material consumption, which is expected to lead to reduced qualification costs (eliminates many costly components and system level qualification tests). Taking the materials design in smaller scale through employing multifaceted approach along with experimental correlation would enhance confidence in the design. Incorporation of multiphase (hybrid) in the atomistic scale broadens up design domain for property tailoring much more than monolithic materials design, where, as stated earlier, the materials interface design constituting the materials hybridization is crucial. This approach would also provide foundations for future efficient and optimal materials design.

Hybrid materials processing at small (nanometer) scale with precise control of materials placement, especially at atomistic scale is not simple, often require meticulously detailed processing science and knowledge of interatomic interaction as microstructure evolves and forms during the process. Another option is to utilize nanoscale materials porosity for materials hybridization by taking advantage of availability of exponentially increasing surface area as pore size goes down. In this case, materials hybridization on materials surface would offer a simpler approach. It is worth to recognize that nanoporous materials construct is not the solution to all application, so, both solid and nanoporous phases should be considered for material hybridization, and is further discussed in the subsequent sections.

In this chapter, the importance and benefit of materials hybridization, especially in the materials interface morphology, at atomic scale are illustrated. A few pervasive examples, common to materials science and mechanics community, are presented to illustrate the approaches to atomic-scale materials interface design in materials hybridization and materials multifunctionality. A broad range of atomistic-, meso-, and macro-scale computational methodologies will be discussed toward atomistic and nanoscale materials design incorporating multiphase (hybrid) materials constructs for tailoring targeted properties. In the subsequent chapters, several materials design approaches are presented for tailoring thermal, electrical, and mechanical properties, and test methods of measuring hybrid materials properties at nano- and submicron scale.

1.2 Example illustrating benefit in atomistic-scale hybrid material interface

1.2.1 Multifunctional durable thermal interface

To illustrate the benefit of employing hybrid materials design at the atomistic scale, let us look the century's old problem of bonded joints. Traditionally, bonded joints are designed for structural components for mechanical load transfer, but they are extremely inefficient in transporting heat across the bonded joint due to poor thermal conductivity of adhesive used in bonded joints. The thermal interface contact junctions in thermal devices on the other hand are designed for efficient thermal transport, but seriously lack in mechanical or structural strength and durability. With respect to these two deficiencies, a bonded joint that can exhibit desirable thermal

Distribution Statement A. Approved for public release (PA): distribution is unlimited.

transport characteristics as well as structural durability, that is, multifunctional (thermal and structural) bonded joint, would overcome these shortcomings. There is substantial benefit in weight and life cycle cost savings in numerous applications if a bonded joint can meet structural as well as thermal performance requirements. Bonded joints are extensively used in space structures, where thermally conductive bonded structural components to mitigate transport of heat generated by actuators, heat exchangers, etc., would eliminate parasite structural components of thermal path needed for transporting heat required for satellite dimensional stability. By space industry's estimate a thermally conductive bonded joint would potentially save \$500k to \$1M life cycle cost per satellite. Similarly, a mechanically robust and structurally durable thermal interface (DTI) would significantly extend performance life of thermal devices and heat exchangers¹⁰. A DTI (bonded joint interface) is depicted in Fig. 1.1, where a design and associated processing protocol were developed¹¹ to incorporate aligned multiwall carbon nanotubes (MWCNT) in the adhesive joint. In this example, the MWCNT provides the thermal transport pathways through the adhesive (poor thermal conductor) phase, and the adhesive bonding provides the structural durability. To create the thermal pathways through the adhesive bond line thickness, contacts of MWCNT [or carbon nanotubes (CNTs)] tips to adhere (in this case is graphite) surface need to be thermally conductive. In other words, the materials morphology of CNT and adherent surface contact (interface) needs to be such that interface thermal contact resistance is minimized. A continuum

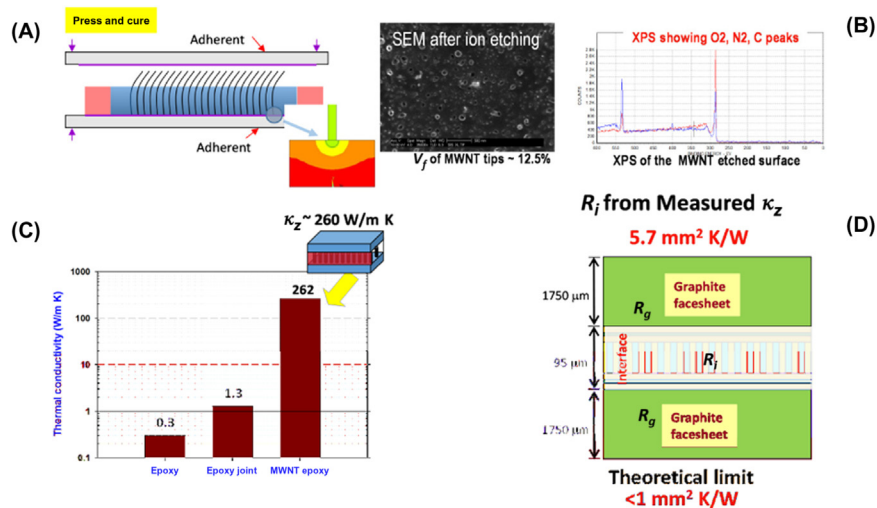


FIGURE 1.1

Durable thermal interface design for thermal and structural (multifunctional) performance. (A) Integration of aligned and tip-metalized MWCNTs across bond thickness, (B) SEM and XPS scan confirm MWCNT tips through the adhesive, (C) measured through-thickness thermal conductivity of traditional and MWCNT (CNT) modified joints, (D) illustration of benefit of optimizing thermal interface design at the atomic scale.

mechanics—based finite element simulation of the CNT/adherent contact for minimizing the thermal interface contact resistance revealed that a metallic contact (a simpler approach than creating a carbon—carbon bonded interface) would yield low interface resistance, see inset next to Fig. 1.1A. Accordingly, per a processing protocol,¹¹ Au-metalized MWCNT tips were bonded with similarly Au-metalized graphite adherent to establish the conductive thermal contacts of MWCNTs with the adherents. Then adhesive was infused to the bond line between the adherents containing MWCNTs (CNTs) and cured to achieve the structural integrity of the joint. The measured through-thickness thermal conductivity (K_z) of the MWCNT-modified bonded joint was over 260 W/m K (cf. Fig. 1.1C) as compared to 1.3 W/m K of traditional (no MWCNT modification) joint—that is, over $200\times$ improvement. This was achieved by establishing the conducting thermal pathways via MWCNTs making conductive thermal contacts with the adherents; the evidence of the metalized MWCNT tips is visible in Fig. 1.1B. *The materials processing step is to establish the MWCNT conductive contacts with adherent surface and infuse the bonding adhesive afterward.* Otherwise, adhesive would ingress in between the MWCNT tips and adherent surface, if adhesive was infused before establishing the MWCNT tip and adherent surface conductive contact. So, this example illustrates that a thermally conductive multifunctional bonded joint is feasible by incorporating conductive (MWCNTs) phase in the bond thickness and making appropriate thermal contact, that is, the MWCNT—adherent interface contact is the key design attribute here. Now, question is, even with $200\times$ improvement of thermal conductivity improvement in this example, whether the interface contact resistance was minimized (or conductance maximized) or not. For this materials composition of Au-metalized MWCNT contact with adherent, from the measured K_z (of 262 W/m K), a simplistic back calculation of MWCNT—adherent interface resistance revealed the interface thermal resistance of $5.7\text{ mm}^2\text{ K/W}$. In comparison, if we further optimize the MWCNT—adherent interface materials composition toward ballistic thermal transport, the interface resistance should be less than $1\text{ mm}^2\text{ K/W}$. To achieve such detailed optimization of interface material composition, we need to do atomistic-scale materials design in which matching of phonon spectra of the constituent materials at the materials interface is needed for optimizing thermal transport characteristics (discussed further in subsequent sections). This also illustrates the beneficial payoff of atomistic-scale material design via materials hybridization.

1.2.2 Carbon nanotube mesh for multifunctional nanocomposites and flexible electronics

There has been a continued ongoing effort of incorporating nanoconstituents such as graphene and CNTs in traditional fiber-reinforced composites for thermal, electrical, or dielectric properties.¹² In addition, networked CNT mesh has been envisioned as a flexible thin film for flexible, stretchable, and wearable sensors and other electronics devices.^{13,14} Fig. 1.2 depicts some of these materials concepts.

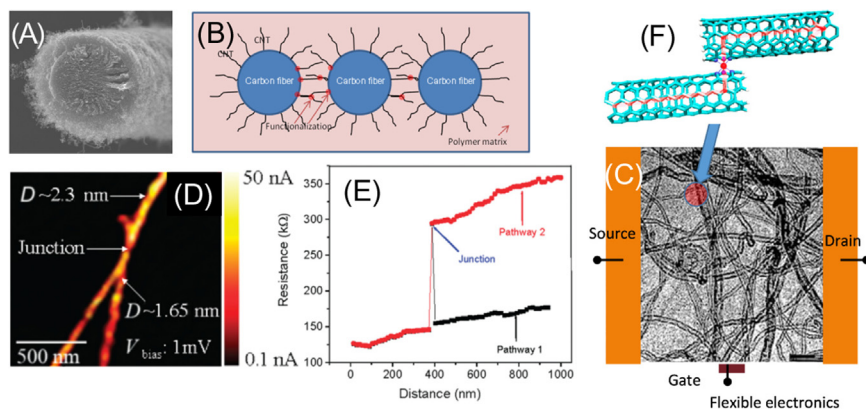


FIGURE 1.2

(A) CNT mesh grown on carbon fiber surface, (B) schematic illustration of CNT-modified multifunctional nanocomposites, (C) CNT mesh flexible electronics, (D) AFM image of electrical resistance tracing, (E) AFM tip thermal resistance tracing, (F) illustration of functionalized CNT–CNT contact.

(D) and (E) Reproduced with permission from Nirmalraj, P.N.; et al. *Electrical Connectivity in Single-Walled Carbon Nanotube Networks*. *Nano Lett.* **2009**, 9(11), 3890–3895.⁹

CNTs grown on carbon fiber (cf. Fig. 1.2A) used to fabricate polymer matrix composites for tailoring thermal, electrical, fracture toughness, etc. The concept of this approach is that when the CNT-modified carbon fibers are assembled and infused in polymer matrix (schematically illustrated Fig. 1.2B), the CNTs would make contacts to create connected pathways for added conductivities (electrical, thermal, etc.). Similarly, thin films of connected network of CNT mesh is a flexible and stretchable materials configuration quite attractive for wearable and conformable sensors and electronics devices^{5,7} (cf. Fig. 1.2C). The materials processing routes adapted in the materials community thus far in embedding the CNT or similar nanomaterials mesh in the polymer phase, either in nanomaterials-modified fiber-reinforced composites or in stretchable polymer thin films, are in general embed or disperse the CNTs or nanomaterials constituents to establish a connected (via nanoelements making surface contacts) network in the polymer phase and then cure the polymer (or matrix) phase. This processing route of curing polymer after the CNT (or nanoconstituent dispersion), as discussed in the prior section, invariably causes polymer to ingress in between the CNT or nanoconstituent contact surfaces, thus, a true CNT–CNT contact is not feasible, rather a CNT–polymer molecule–CNT contact is formed (cf. Fig. 1.2F). Molecular Dynamics (MD) calculations reveal that the presence of a polymer molecule in between the CNT–CNT contact substantially increases the contact resistance.¹⁵ As a result, in such processing approaches success in enhancing either the electrical or thermal conductivity has been limited¹⁶ due to the fact that the materials morphology at the contact is

not optimized for desired contact conductivity enhancement. Related to optimizing the contact resistance (or conductance), even in the case of van der Waals surface contacts (i.e., absence of any functionalizing molecules in between the contact surfaces), atomic force microscopy (AFM) measurement implies that a significant contact resistance exists, which could be as high as 10^6 times of that of CNT's inherent resistance⁹ (cf. Fig. 1.2D and E). Fig. 1.2D and E shows the AFM trace data along the CNT length. It is to note that, as the AFM tip traces one CNT to another through the contact, there is steep jump in the resistance data at the contact location (cf. Fig. 1.2E), confirming the existence of high contact resistance even in the van der Waals contact. To effectively utilize CNTs or any other nanoconstituents in real-world device design, due to its finite dimensions, connected CNTs (or nanoconstituent) via appropriately design contacts (interface) are a practical way to go. Hence, the optimization of interface material morphology at contact point becomes so important for enhancing or tailoring the device performance.

1.2.3 Approaches for nanomaterials interface materials selection and its design

Interface materials performance characteristics at contact points of nanomaterials, as stated earlier, strongly influence the overall nanomaterials performance. The interface van der Waals contacts of nanoconstituents or CNTs for materials design may be adequate for certain applications, but found to be not sufficient for robust device performance, such as for stretchable and flexible devices subjected to high strain. Ideally, fused junctions of the same atomic composition of the nanoconstituents are desirable, but often that is practically not feasible with nanomaterials. Alternatively, a feasible approach is to modify van der Waals contacts with selected molecular functionalization (i.e., covalently attaching desired molecules) at the contact interface. For CNTs or graphene flakes, both polymeric and metallic molecules are extensively studied for interface functionalization. However, selection of such interface functionalizing molecules would depend on the desired interface performance characteristics. For example, molecules that would be ideal for tailored thermal conductance at the interface may not work well for electrical or structural performance. In this section, interface functionalization for thermal conductance with polymer molecules and then that with metallic molecules, its respective advantages and disadvantages, will be discussed.

1.2.3.1 Interface functionalization with polymeric molecules

The materials processing associated with interface functionalization with polymeric molecules is quite popular, convenient, and perceived to be low cost as compared to its metallic alternative. However, random insertion of any given molecule would not yield the desired interface performance characteristics. To elaborate this point, materials selection for tailoring thermal conductance is first discussed, followed by that for metallic molecules for CNT interface junction (contact) functionalization. The detailed analysis for the physics of interface

thermal conduction tailoring is presented in Chapter 2. In Fig. 1.3, a case of CNT–CNT contact interface thermal conductance using polymeric molecules for the contact interface functionalization is presented. In this example, the thermal transport occurs across its side-wall contact of two parallel CNTs, embedded in a polymer matrix. One of the CNTs (red) is heated and the thermal energy is taken out through the cold (blue) CNT (cf. Fig. 1.3A). In this simulation, performed using MD, the interface thermal energy transport took place across the CNT side-wall surfaces that are closest to each other (i.e., in contact). As expected, with increasing number of surface functionalization sites with CH_2 molecules, the interface temperature difference between the hot and cold CNTs goes down, which means its interface contact thermal conductance is increasing (cf. Fig. 1.3C). Although the interface conductance increases with increasing the functionalization sites (degree of functionalization) with CH_2 , however, we need to explore if CH_2 is the molecule of choice or not. It is known that the interface thickness (i.e., separation distance between the two CNT walls, in this case) and the functionalizing molecule properties (stiff or soft) influence the interface thermal conductance. A set of polymer molecules (CH_2 , C_3H_6 , C_5H_{10} , benzene, and Epon) of varied molecular length and stiffness (rigidity) were analyzed to assess

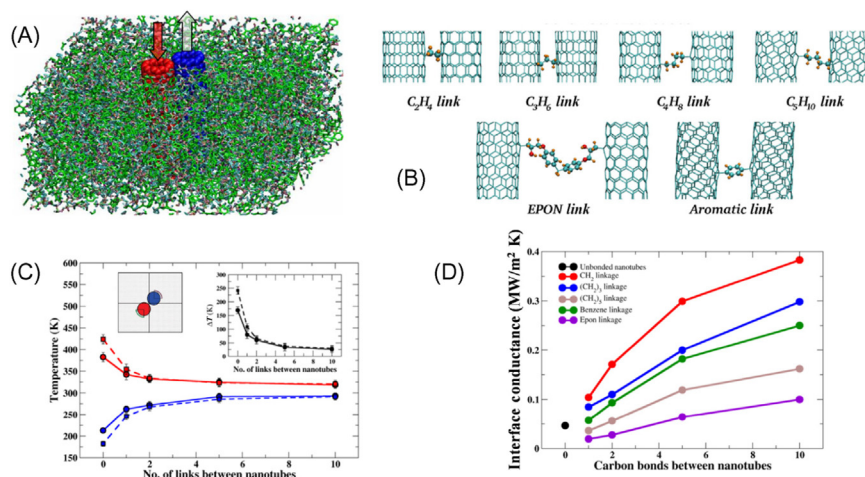


FIGURE 1.3

(A) Schematics of two parallel CNTs next to each other one being heated, thermal energy transport takes place across the CNT contact surface, (B) CNT side walls are functionalized (linked) with various polymer molecules (short, long, stiff, and soft), (C) interface temperature difference between hot and cold CNTs with increasing functionalization (linkers), (D) interface thermal conductance for various linkers, black dot represents van der Waals contact.

All four plots reproduced from Varshney, V.; et al. *Modeling of Thermal Conductance at Transverse CNT–CNT Interfaces*. *J. Phys. Chem. C* **2010**, 114(39), 16223–16228¹⁵; Sihm, S.; et al. *Prediction of 3D Elastic Moduli and Poisson's Ratios of Pillared Graphene Nanostructures*. *Carbon* **2012**, 50(2), 603–611.¹⁷

their effect on the interface conductance (cf. Fig. 1.3B—the schematics of CNT side-wall functionalization with different polymer molecules).¹⁵ The calculated interface thermal conductance with above set of functional molecules with varied degree of functionalization, reproduced from Ref. [15], is shown in Fig. 1.3D. The values of the interface thermal conductance of the respective functionalizing molecules are shown with reference to the nonbonded (i.e., van der Waals contact) shown as a black solid circle in Fig. 1.3D. It can be inferred from the data that any type of chemical functionalization would not always yield improvement in the interface conductance. As seen in Fig. 1.3D, at low degree of functionalization with Epon and C₅H₁₀ molecules degrades the interface conductance as compared to that of nonbonded contact. This is primarily due to the fact that these two molecules are longer as compared to the other molecules, causing larger separation between the CNTs, hence contributed to conductance reduction. Whereas, the relatively smaller length and stiffer molecules (such as CH₂ and benzene) offer relatively better improvement in interface conductance. However, although a 7–8 × improvement in the interface thermal conductance was achieved with these polymer molecule functionalization as compared to that of noncovalent (van der Waals) interface (~0.05 MW/m² K), it was essentially limited to around 0.4 MW/m² K, which is essentially attributed to poor thermal transport properties of polymer. For further enhancement of interface conductance, metallic nanoparticle (known to be several order of magnitude conductive than polymers) functionalization offers promising potential, which is discussed in the next section.

1.2.3.2 Interface functionalization with metallic nanoparticles

The interface thermal transport in metallic medium is conveniently analyzed by the phonon (carrier of the thermal energy) spectrum. Due to covalent bonding of polymer atoms and random polymer chain distribution in its microstructure, the associated phonon spectra span a wide frequency range (theoretically known to have infinite frequency domain). On the other hand, atoms in metals are not covalently bonded and because of its ordered microstructure its associated phonon spectrum frequency spread is limited and associated upper frequency limit is known as Debye frequency (also, commonly known as Debye temperature). For the interface thermal conductance, G , the extent of overlap of the phonon vibrational density of states (VDOS) between the two materials phases at the interface (e.g., CNT and metal nanoparticles in CNT/nanometal interface) determines the value of G . The interface thermal conductance, G , is defined as,¹⁸

$$G = \int_w k_B \chi(\omega) \Phi_1(\omega) \Phi_2(\omega) \left(\frac{h\omega}{k_B T} \right)^2 \frac{\exp\left(\frac{h\omega}{k_B T}\right)}{\left[\exp\left(\frac{h\omega}{k_B T}\right) - 1 \right]^2} d\omega \quad (1.1)$$

where $\Phi_1(\omega)$ and $\Phi_2(\omega)$ are the VDOS of the two phases and $\chi(\omega)$ is the coupling function (averaged over all polarizations), and other symbols in Eq. (1.1) have their usual meaning. It is to note that the major heat carrier through van der Waals interface (nonbonded interface between CNTs and nanometal) is

characteristically the low-frequency vibrations that are around 5–7 THz, above which $\chi(\omega)$ decays quickly for higher frequencies.¹⁸ This justifies the use of classical simulations, such as MD for calculating the interface conductance of soft interfaces (such as metallic interface; in comparison, the ceramic materials interface would be considered as hard interface). MD simulation only captures the phonon contribution. In metallic interface, however, in addition to phonons, there is a contribution due to electron scattering to the overall interface thermal conductance. The electronic contribution can be easily estimated with standard closed form equations available in many handbooks; thus is not repeated here.

Fig. 1.4 is an illustration of CNT's metallic interface conductance mechanism and design case. For metallic materials selection for the interface, the phonon VDOS spectra of fullerenes, CNTs, and a few common metallic nanoparticles (Au, In, Cu, Al) are shown in Fig. 1.4. As stated earlier, the overlap of the VDOS spectra of the interface materials influences the interface thermal conductance. If we want to use fullerenes (C₆₀, etc.) instead of CNTs for the purpose of tailoring conductivity in composite materials with metallic functionalization, there is serious limitation of enhancing the interface conductance due to the fact that the overlap of the VDOS frequency between fullerenes and metallic nanoparticles is very limited (cf. Fig. 1.4). Nanometals possess low-frequency VDOS, whereas fullerenes exhibit high-frequency VDOS due to its caged spherical carbon bond structure (zero-dimensional). In

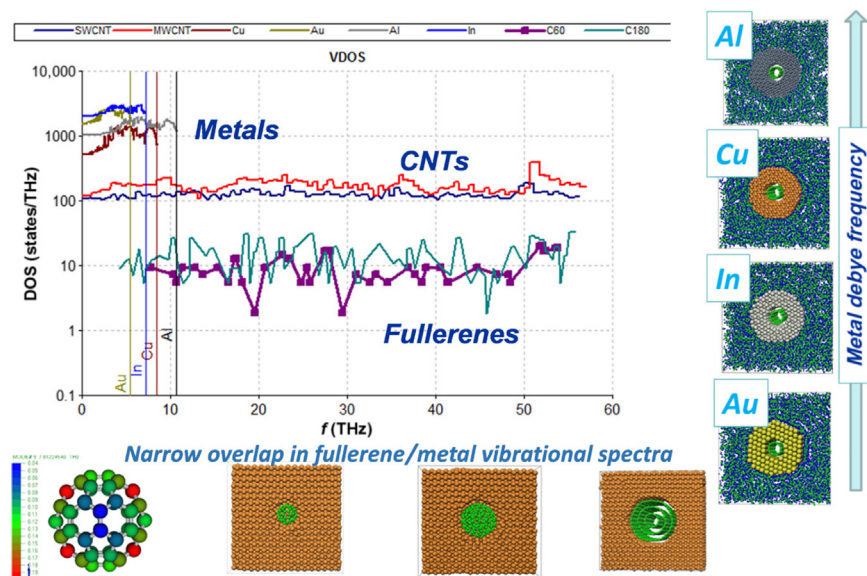


FIGURE 1.4

Comparison of phonon vibrational spectra density of state (DOS) comparison of CNTs and fullerenes with different metallic interfaces.

Reproduced from Shenogin, S.; et al. *Molecular Dynamics Studies of Thermal Boundary Resistance at Carbon–Metal Interfaces*. *Scr. Mater.* **2013**, 69(1), 100–103.¹⁸

comparison, one-dimensional CNT's VDOS spectra cover a wide range (low to high frequency) and hence fully overlap the nanometal VDOS (cf. Fig. 1.4). As a result, for metallic interface functionalization, CNTs are preferred over fullerenes for tailoring thermal conductance in composites. Even in metallic functionalization, the metal that exhibits higher VDOS spectra overlaps with that of CNTs would be preferred for enhancing the interface conductance. For example, Al would be preferred as compared to either Au, Cu, or In (cf. Fig. 1.4). Such relative interface thermal conductance was experimentally validated by measuring the interface thermal conductance of highly oriented pyrolytic graphite coated with metal nanoparticles with plasma vapor deposition (PVD). The measured interface conductance is shown in Fig. 1.5, whose trend agrees well with the VDOS study. Worth to note that the MD prediction of the interface conductance consistently under predicted the measured data by about 10–20 MW/m² K. This difference is attributed due to the electronic contribution, which was not feasible to capture in MD simulation. In general, the electronic contribution of graphite-Cu interface thermal conductance is estimated to be around 22 MW/m² K, so, if you add this value to the MD predictions of all the metal cases considered here, the predicted interface thermal conductance compared well with that of the measured data (cf. Fig. 1.5). Further, in this example, with metallic functionalization over 100× interface conductance enhancement was achieved as compared to nonbonded (van der Waals) interface, which was 10–15× superior to that of polymer functionalization. Thus metallic interface functionalization is an appealing option for interface material design and hybrid materials property tailoring. The PVD approach can be easily used to coat CNTs or nanocarbon fibers (cf. Fig. 1.5—right image, Au nanoparticle-coated nanocarbon fibers by PVD). A heat treatment of such nanoparticle-coated CNT mesh would produce fused metallic CNT junctions

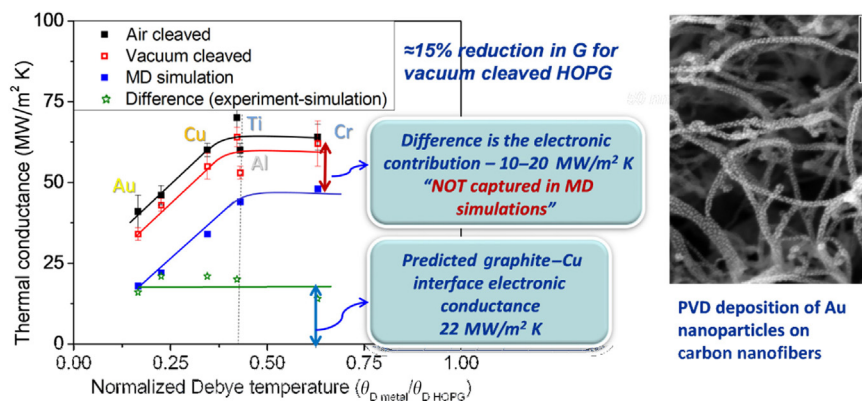


FIGURE 1.5

Comparison of predicted and measured interface thermal conductance of a few metallic interfaces on graphitic surface. Thermal conductance by TDTR includes contribution of both phonons and electrons.

Reproduced from Shenogin, S.; et al. *Molecular Dynamics Studies of Thermal Boundary Resistance at Carbon–Metal Interfaces*. *Scr. Mater.* **2013**, 69(1), 100–103.¹⁸

that are flexible, stretchable, and mechanically robust for multifunctional composite application.

A similar material design approach is equally applicable for tailoring electrical conductance (for electronic properties) for hybrid materials using Tight-Binding Non-equilibrium Green Function (TB-NEGF) methodology,¹⁹ which is covered in a separate chapter later in this book.

1.3 Nanoporous carbon materials—advantages of atomistic-scale porous morphology

In addition to optimal interface design for hybridization in solid materials form, nanoporous materials morphology is another materials construct that offers enormous potential for efficient material hybridization and enhanced performance efficiency. The real advantage of nanoscale materials porosity for materials hybridization is the availability of exponentially increasing surface area as pore size goes down. In this case, the open-pore surface materials hybridization could be easily done by taking advantage of mature materials infiltration, surface coating techniques such as PLD, PVD, magnetron sputtering, and many more.

The advantage of surface area increase with decreasing pore size of spherical pores embedded in a material volume is illustrated in Fig. 1.6. The schematics of a cross-sectional view (a cut across the great circle of symmetrically aligned pore spheres) are shown in Fig. 1.6A, which implies that as the pore size decreases at same overall pore volume fraction (i.e., pore fractal number, m , increases) the surface area in a given volume increases dramatically. A quantitative representation of the surface area to volume ratio (S/V ratio) with varying pore fractal number, m , and pore volume fraction, p_f , is shown in Fig. 1.6B. Here, for simplicity, the S/V ratio data is shown with calculation limited to pore sizes such that adjacent pore surfaces at most make point contacts. As it is easily inferred from the two plots of S/V data, one with increase pore fractal number in semi-log scale and the other in linear scale with increasing pore volume fraction, there is a great opportunity of utilizing the enormous availability of surface area for materials hybridization and materials functionality as the pore size decreases. In addition, for open-cell porous medium, the pore volume fraction would be even higher than the data shown and consequently, associated S/V value would be even higher than what is shown here. So, nanoporous materials enormously expand the geometric domain for materials multifunctionality and hybridization.

A design of an open-cell nanoporous carbon material form, hybridizing CNTs, and graphene layers is shown in Fig. 1.7. A junction of CNT aligned perpendicular to graphene surface is thermodynamically stable.²² In creating such CNT–graphene junction shown in Fig. 1.7A and B, six heptagonal (seven-member) carbon rings, in addition to another six hexagonal carbon rings, are needed to form the CNT–graphene junctions around the junction circumference. The middle red heptagonal ring in Fig. 1.7B is one such heptagonal ring present in CNT–graphene junction. Creation of such CNT–graphene junctions has been demonstrated in the literature

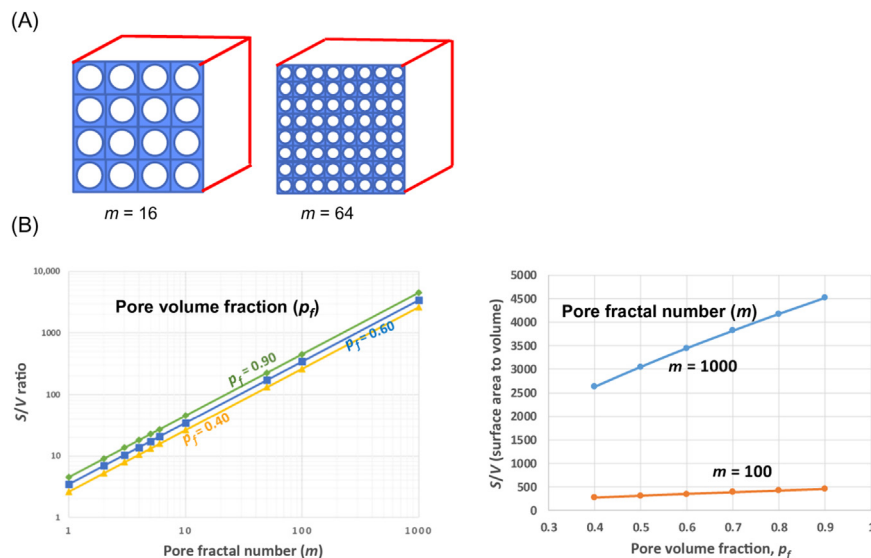


FIGURE 1.6

(A) Schematics of increasing surface area per unit volume with decreasing pore size and increasing pore fractal number (m). (B) Plots of surface area to volume ratio with increasing pore fractal number (m) and pore volume fraction (p_f) in semi-log and linear scale, respectively.

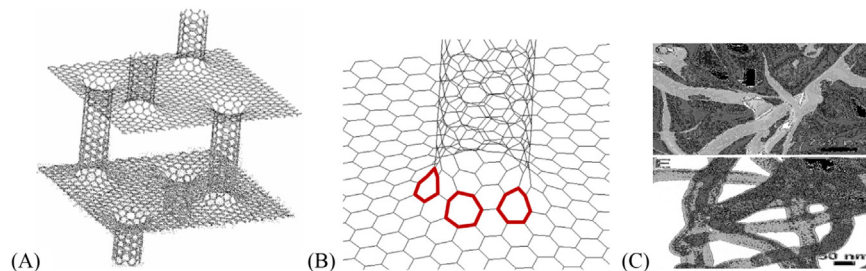


FIGURE 1.7

Graphene and CNT hybrid nanoporous carbon material form. (A) Simulation image of a set of distributed CNTs junctioned perpendicular to graphene layers to form open-cell nanoporous carbon, (B) one of the six heptagon (seven-member) carbon rings shown, in addition to regular hexagonal rings, to form CNT-graphene junctions,^{17,20} (C) a similar CNT-CNT junctioned nanoporous carbon CVD process.

Reproduced from Hashim, D.P.; et al. Covalently Bonded Three-Dimensional Carbon Nanotube Solids via Boron Induced Nanojunctions. *Sci. Rep.* **2012**, *2*, 363.²¹

[23] for supercapacitors and other applications. In addition, processing scheme such as chemical vapor deposition (CVD) with doping agents to create CNT–CNT junctions in real time during the CNT growth process has also been successfully developed²¹ (cf. Fig. 1.7C). Besides these two processing approaches, there are many other similar processing schemes developed by many research groups around the world to make nanoporous hybrids, such as metal organic framework and graphene organic framework, which open up unprecedented material design domain for materials hybridization and multifunctionality of tailored properties. In Fig. 1.8 a few forms

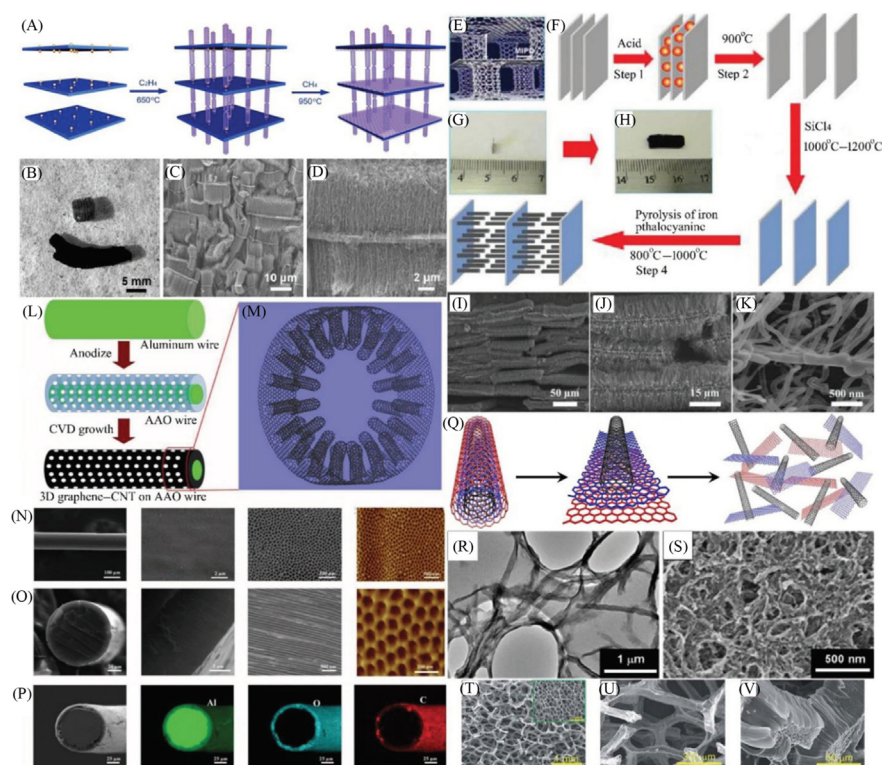


FIGURE 1.8

(A–H) Schematics and synthesis of aligned CNT/graphene sandwiches on bifunctional porous graphene sandwiches, (I–K) SEM images of 3D pillared VACNT–graphene nanostructures, (L and M) schematics of synthesis procedure and 3D graphene–CNT hybrid, (N–P) nanoporous surface RACNT fiber’ SEM and EDX elemental mapping, (Q) assembly of CNTs of varying diameters in nano porous structures, (R–V) TEM and SEM images of porous graphene/CNT hybrids.

Reproduced with permission Paul, R.; et al. *Integrated Energy Devices: 3D Heteroatom-Doped Carbon Nanomaterials as Multifunctional Metal-Free Catalysts for Integrated Energy Devices*. *Adv. Mater.* **2019**, 31 (13), 1970094.²⁴

of nanoporous carbon materials for ultra-energy-efficient supercapacitors and other applications are shown.

Multiple materials processing approaches have been employed to achieve different nanoporous morphology composing of different hybrid material constructs (cf. Fig. 1.8). For the layered nanoporous sandwich form of aligned CNTs in between layers of porous graphite sheets processing steps involved CNT grown on graphite surface by CVD and then transferred to form layered nanoporous CNT/graphite stack (cf. Fig. 1.8A–H). Nanohole templated anodized aluminum oxide for simultaneous graphene and CNT growth by CVD to create integrated 3D graphene/CNT structure is another example (cf. Fig. 1.8M). The microstructures and chemical composition (EDX) of other types of nanoporous hybrids undergoing heteroatom hybridization and postprocessing pyrolysis for special battery electrodes (cf. Fig. 1.8N–V) are a few examples of realizing a variety of nanoporous materials constructs that would open a new domain of materials design space.

1.4 Mesoscale materials modeling needs for efficient device design

Materials modeling integration with processing science is essential for accelerated materials innovation, development, and its transition to product design. In order for nanoscale materials design attributes to effectively contribute to the device performance, it is a well-known fact that atomistic materials modeling tools are to be integrated with device scale (i.e., continuum scale) tools (schematically depicted in Fig. 1.9). Tool integration covering such a wide range is not simple. A stepwise comprehensive approach needs to be pursued in which intermediate steps of set of mesoscale tools are to be integrated to bridge the atomistic to continuum domains. Although modeling tools in the atomistic and continuum domains are well developed, however, progress in validated mesoscale materials modeling tool set is still lacking. Experimentally validated scalable mesoscale computational tools, such as Lattice Boltzmann Equation, DFT Tight Binding (DFTB), and Kinetic Monte Carlo, are necessary, for example, to closely integrate processing simulation with evolving materials properties during materials processing. An integrated approach like this would accelerate materials development at a faster pace and would substantially eliminate the trial and error approach of material processing. To illustrate this point, the materials growth kinetics of epitaxial graphene layer on *h*-BN surface is shown in Fig. 1.10. There are a lot of materials process variables that influence the epitaxial growth kinetics on graphene layer, such as temperature, pressure, formation energy, and carbon atomic state, to control material stoichiometry of the growing layer. By employing a self-consistent charge DFT Tight Binding (SCC-DFTB) methodology, it was demonstrated that a trimer carbon, as compared to

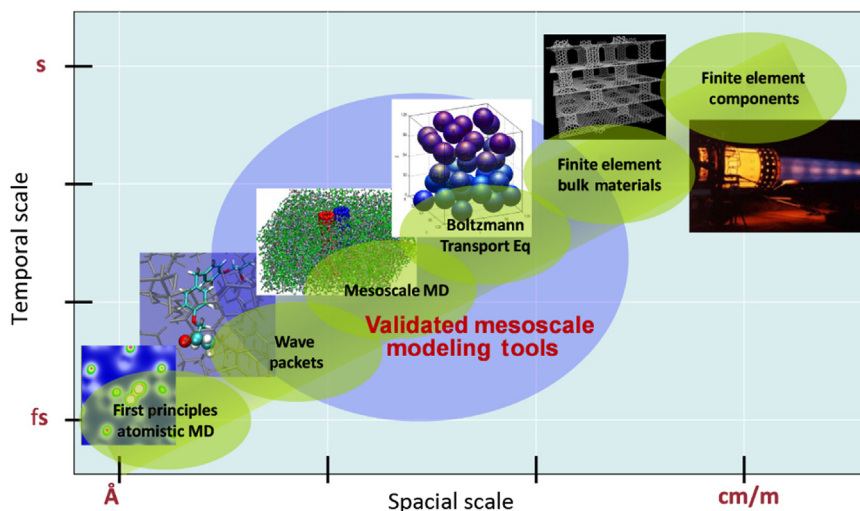


FIGURE 1.9

A notional scheme for multiscale (both spatial and temporal domain) materials modeling integration, particularly the need for validated mesoscale modeling tools.

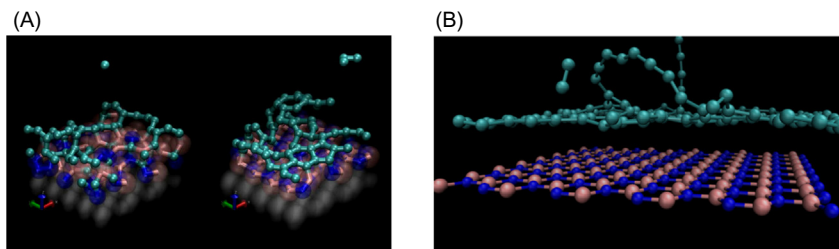


FIGURE 1.10

Simulation of graphene growth on h-BN surface using SCC-DFTB, (A) the effect of formation energy state of atomic and trimer carbon on the growth kinetics, (B) initial formation state of graphene layer on h-BN surface—trimer carbon favors such formation.²⁵

atomic carbon, would be the preferred molecular state for the epitaxial graphene growth.²⁵ The deposition chamber temperature, pressure, etc., should thus be tuned for trimer-type carbon, not creation of atomic carbon, to enable such controlled epitaxial graphene growth. Thus a mesoscale computational methodology like this one is an example of how materials development cycle can be accelerated and would also potentially lower materials discovery and developmental cost.

1.5 Conclusions

Hybrid materials design is an attractive materials design approach for efficient materials use and it exceedingly expands the materials design space. The optimal materials interface design on materials hybridization is critical in tailoring the materials functional attributes. Further, as we take the materials hybridization to small scale, the materials optimization, materials use efficiency, and performance merit improve accordingly. Thus there is a compelling benefit that efficiently connects the atomistic-scale materials attributes to device performance, for which vetted (experimentally validated) mesoscale computational tools would facilitate such effective connection.

References

1. Mangalam, A. P.; Simonsen, J.; Benight, A. S. Cellulose/DNA Hybrid Nanomaterials. *Biomacromolecules* **2009**, *10* (3), 497–504.
2. Taylor-Pashow, K. M. L., et al. Hybrid Nanomaterials for Biomedical Applications. *Chem. Commun.* **2010**, *46* (32), 5832–5849.
3. Morris, R. E.; Wheatley, P. S. Gas Storage in Nanoporous Materials. *Angew. Chem. Int. Ed.* **2008**, *47* (27), 4966–4981.
4. Ngo, T. D., et al. Additive Manufacturing (3D Printing): A Review of Materials, Methods, Applications and Challenges. *Compos. Part. B: Eng.* **2018**, *143*, 172–196.
5. Heo, J. S., et al. *Recent Progress of Textile-Based Wearable Electronics: A Comprehensive Review of Materials, Devices, and Applications.* *Small* **2018**, *14* (3), 1703034.
6. Werner, M. R.; Fahrner, W. R. Review on Materials, Microsensors, Systems and Devices for High-Temperature and Harsh-Environment Applications. *IEEE Trans. Ind. Electron.* **2001**, *48* (2), 249–257.
7. Zeng, W., et al. Fiber-Based Wearable Electronics: A Review of Materials, Fabrication, Devices, and Applications. *Adv. Mater.* **2014**, *26* (31), 5310–5336.
8. Wallace, G.G., et al. Smart Nanotextiles: A Review of Materials and Applications. **2007**, <https://ro.uaw.edu.au/scipapers/1232>.
9. Nirmalraj, P. N., et al. Electrical Connectivity in Single-Walled Carbon Nanotube Networks. *Nano Lett.* **2009**, *9* (11), 3890–3895.
10. Roy, A. K., et al. Importance of Interfaces in Governing Thermal Transport in Composite Materials: Modeling and Experimental Perspectives. *ACS Appl. Mater. Interfaces* **2012**, *4* (2), 545–563.
11. Ganguli, S., et al. Metalized Nanotube Tips Improve Through Thickness Thermal Conductivity in Adhesive Joints. *J. Nanosci. Nanotechnol.* **2008**, *8* (12), 7.
12. Cui, X., et al. Thermal Conductive and Mechanical Properties of Polymeric Composites Based on Solution-Exfoliated Boron Nitride and Graphene Nanosheets: A Morphology-Promoted Synergistic Effect. *ACS Appl. Mater. Interfaces* **2015**, *7* (34), 19068–19075.
13. Ha, M.; Lim, S.; Ko, H. Wearable and Flexible Sensors for User-Interactive Health-Monitoring Devices. *J. Mater. Chem. B* **2018**, *6* (24), 4043–4064.

14. Guo, F., et al. Stretchable and Compressible Strain Sensors Based on Carbon Nanotube Meshes. *Nanoscale* **2016**, *8* (46), 19352–19358.
15. Varshney, V., et al. Modeling of Thermal Conductance at Transverse CNT – CNT Interfaces. *J. Phys. Chem. C* **2010**, *114* (39), 16223–16228.
16. Mrozek, R. A.; Lenhart, J. L.; Slipher, G. A. Deformable Polymer Composites with Controlled Electrical Performance During Deformation Through Tailored Strain-Dependent Conductive Filler Contact. Google Patents, 2017.
17. Sihn, S., et al. Prediction of 3D Elastic Moduli and Poisson’s Ratios of Pillared Graphene Nanostructures. *Carbon* **2012**, *50* (2), 603–611.
18. Shenogin, S., et al. Molecular Dynamics Studies of Thermal Boundary Resistance at Carbon–Metal Interfaces. *Scr. Mater.* **2013**, *69* (1), 100–103.
19. Shenogin, S.; Ferguson, L.; Roy, A. K. The Effect of Contact Resistance on Electrical Conductivity in Filled Elastomer Materials. *Polymer* **2020**, 122502.
20. Varshney, V., et al. Modeling of Thermal Transport in Pillared-Graphene Architectures. *ACS Nano* **2010**, *4* (2), 1153–1161.
21. Hashim, D. P., et al. Covalently Bonded Three-Dimensional Carbon Nanotube Solids via Boron Induced Nanojunctions. *Sci. Rep.* **2012**, *2*, 363.
22. Dimitrakakis, G. K.; Tylianakis, E.; Froudakis, G. E. Pillared Graphene: A New 3-D Network Nanostructure for Enhanced Hydrogen Storage. *Nano Lett.* **2008**, *8* (10), 3166–3170.
23. Du, F., et al. Preparation of Tunable 3D Pillared Carbon Nanotube–Graphene Networks for High-Performance Capacitance. *Chem. Mater.* **2011**, *23* (21), 4810–4816.
24. Paul, R., et al. Integrated Energy Devices: 3D Heteroatom-Doped Carbon Nanomaterials as Multifunctional Metal-Free Catalysts for Integrated Energy Devices. *Adv. Mater.* **2019**, *31* (13), 1970094.
25. Lee, J., et al. In Silico Carbon Molecular Beam Epitaxial Growth of Graphene on the h-BN Substrate: Carbon Source Effect on van der Waals Epitaxy. *Nanoscale* **2016**, *8* (18), 9704–9713.